

Demonstration of Feeding Vehicle-Integrated Photovoltaic-Converted Energy into the High-Voltage On-Board Network of Practical Light Commercial Vehicles for Range Extension

Robby Peibst, Hilke Fischer, Manuel Brunner, Andreas Schießl, S. Wöhe, Reinhard Wecker, Felix Haase, Henning Schulte-Huxel, Susanne Blankemeyer, Marc Köntges, Christina Hollemann, Rolf Brendel, Gustav Wetzels, Jan Krügener, Hermann Nonnenmacher, Heiko Mehlich, Andrei Salavei, Kaining Ding, Andreas Lambertz, Bart Pieters, Stefan Janke, Bernd Stannowski, and Lars Korte*

The setting up of a practical electrically driven light commercial demonstration vehicle with integrated photovoltaics (PV) is reported. The demonstrator vehicle is equipped with 15 modules based on the crystalline Si/amorphous Si heterojunction technology. The nominal total peak power under standard testing conditions is 2180 W_p. Specifically, the PV-converted energy is fed into the high-voltage (HV; 400 V) board-net for a utilization of the large capacity of the HV battery and thus for direct range extension. The demonstrator vehicle is equipped with irradiation, wind, temperature, magnetic, and global positioning system sensors. Irradiation and temperature as well as the energy flows from modules, maximum power point trackers (MPPTs), low-voltage buffer battery to HV battery via DC/DC, and from the HV battery to the loads during an exemplarily test drive day (May 31, 2021) are monitored. The range extension obtained at this day on our test route (51° 59' N, 9° 31' E) was 36 km, the corresponding CO₂ savings account for ≈2.3 kg. The chain efficiency of the electronic components from the input side of the MPPTs to the HV output side of the DC/DC was 68.6%, whereas the DC/DC itself has an average efficiency of 90%.


1. Introduction

While the integration of photovoltaics (PV) into electrically driven vehicles has been demonstrated already in 1960,^[1] vehicle-integrated PV (VIPV) is recently gaining increasing attention. This approach can contribute to the reduction of the emission of greenhouse and other harmful gases.^[2–4] In addition, VIPV has the potential to reduce peak loads for the electric grid and to provide balance energy.

For light commercial vehicles (LCVs), the rather high cuboid compartment provides a rather large area for PV while the energy consumption for driving is still comparable to that of passenger cars. Requirements on aesthetics such as curvature of the PV modules are relaxed. Furthermore, the drive pattern for LCVs probably include sufficiently long on-board PV-based recharging periods. We therefore

R. Peibst, H. Fischer, F. Haase, H. Schulte-Huxel, S. Blankemeyer, M. Köntges, C. Hollemann, R. Brendel
Institute for Solar Energy Research Hamelin (ISFH)
31860 Emmerthal, Germany
E-mail: peibst@isfh.de

H. Nonnenmacher, H. Mehlich
Meyer-Burger Germany
An der Baumschule 6-8
09337 Hohenstein-Ernstthal, Germany

 The ORCID identification number(s) for the author(s) of this article can be found under <https://doi.org/10.1002/solr.202100516>.

© 2021 The Authors. Solar RRL published by Wiley-VCH GmbH. This is an open access article under the terms of the Creative Commons Attribution-NonCommercial-NoDerivs License, which permits use and distribution in any medium, provided the original work is properly cited, the use is non-commercial and no modifications or adaptations are made.

DOI: 10.1002/solr.202100516

M. Brunner, A. Schießl
Vitesco Technologies
93055 Regensburg, Germany

S. Wöhe, R. Wecker
a2-solar Advanced and Automotive Solar Systems
99099 Erfurt, Germany

R. Peibst, G. Wetzels, J. Krügener
Institute for Electronic Materials and Devices
Leibniz University of Hannover
30167 Hannover, Germany

A. Salavei, K. Ding, A. Lambertz, B. Pieters
Institute for Energy and Climate Research 5
Forschungszentrum Jülich (JÜLICH)
52425 Jülich, Germany

S. Janke, B. Stannowski, L. Korte
Helmholtz Zentrum Berlin (HZB)
14109 Berlin, Germany

expect that for electric-driven LCVs, the economic viability of VIPV can be achieved earlier than for passenger cars. Recent commercial announcements^[5,6] seem to confirm the attractiveness of this specific VIPV application.

So far, VIPV has been applied in “practical vehicles” mainly for indirect on-board functions such as cooling (e.g., for truck trailers)^[7–9] or air conditioning. In this case, the PV-generated electricity is fed into the low voltage (LV; 12 or 48 V) on-board network with a rather limited battery capacity <1 kWh.

To also utilize PV-converted energy for driving and thus for reduction of charging events from the grid,^[10] it is required to feed it into the high voltage (HV, 400 or 800 V) on-board network. This approach also has the advantage that the large capacity of the HV battery can be accessed to store all PV-converted energy, e.g., when charging during parking times. For this purpose, a well-designed buck-boost DC/DC converter from the typical output voltage of maximum power point trackers (MPPTs) at 12 V to the 400 V (or 800 V) level with a smart operation strategy, a high conversion efficiency and low standby power consumption is required. Safety issues and possible interferences with critical driving functions have to be considered when interfacing to the HV on-board network. Furthermore, all other components of the vehicle-integrated PV system need to be adapted for this specific application: solar cells have to be as efficient as possible due to space constraints and to exhibit a low temperature coefficient, solar modules need to be robust against mechanical stress, lightweight and tolerant against dynamic partial shading, and the on-board electronic has to track the maximum power point sufficiently fast.

Here, we report on Continental Engineering Services, a2-solar, Vitesco, HZB, JÜLICH, MBE, Meyer–Burger and ISFH joining their expertise in their respective working fields, addressing the abovementioned challenges, and setting up a practical demonstration vehicle based on the Streetscooter WORK L electrically driven LCV. We report on the energy flow in our demonstrator vehicle for an exemplary test drive day, analyzing both the resulting range extension as well as the efficiencies of the single components.

Eventually, this work intends to contribute to an experimental verification of an as significant as projected^[4] contribution from on-board PV-converted energy.

2. Experimental Section

2.1. VIPV Demonstrator Vehicle

For the solar cells, we choose the crystalline Si technology based on high-efficient a-Si:H/c-Si heterojunction (SHJ) double-side contacted cells from Meyer–Burger Germany. The temperature coefficient for the efficiency of these cells is—thanks to the high open-circuit voltage >740 mV—only $-0.2\% \text{ K}^{-1}$. Although we acknowledge that also III–V-based cells with even higher efficiencies were evaluated for VIPV applications,^[11] we think that highly efficient crystalline Si solar cells posed a good compromise between energy yield and costs. ISFH assembled these cells to strings by using the In-free Smart Wire Technology from Meyer–Burger. Besides many other positive aspects, one major advantage of this concept for the application in VIPV is mechanical robustness and its tolerance against microcracks in the solar cells. The strings are integrated into 15 glass-based modules by a2-solar with a total area of 11.6 m^2 ^[12]. Four modules are mounted on each side, five on the roof, and two on the rear. The total peak power under STC is 2180 W_p , where the modules mounted on the roof (sides and rear) of the compartment account for 875 (1305) W_p . Fast MPPTs and the buck-boost DC/DC converter are developed by Vitesco. We use ten MPPTs while wiring two modules on the side and rear to one MPPT in series, respectively. We furthermore mount four irradiation sensors (front, rear, left, right), a wind sensor, a global positioning system sensor, a temperature sensor, and magnetic sensor.^[13] All VIPV components are integrated in the electrically driven LCV model “WORK L” from Streetscooter by Continental Engineering Services under consideration of all safety aspects. A MicroAutoBox controls the system and sends all status data of the vehicle as well as the data from the sensors to a datalogger to monitor the entire energy flow in the vehicle. **Figure 1** shows photographs of essential details of the demonstrator vehicle. The demonstrator vehicle obtained road permission.

Figure 2 shows the block diagram of the VIPV components. The energy flow in the system is the following: After PV energy conversion in the PV modules, the energy is transferred to the MPPTs. From here, a major amount of the energy is stored intermediately in a LV (12 V) buffer battery. The intention here

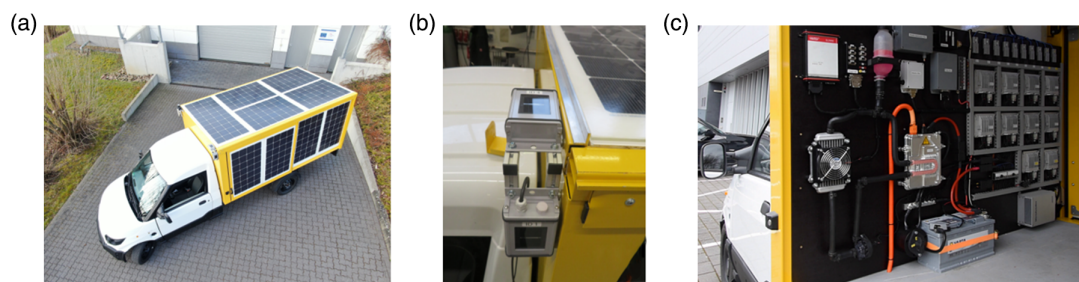


Figure 1. Photographs of a) the demonstration vehicle, showing the PV modules integrated in the sides and in the roof of the compartment, b) the irradiation sensors facing up and to the left, mounted on the top of the front side of the compartment, c) electronic VIPV components mounted on the inner front side of the compartment. The essential buck-boost DC/DC converter is located in the box connected to the orange high voltage cable.

Figure 2. Block diagram of VIPV components (modules = blue, MPPTs, DC/DC and MABox = orange), sensors (yellow) and data logger integrated in the Streetscooter WORK L demonstration vehicle.

Since April 2021, we perform daily test drives. We use a long commuter route with a total length of ≈ 60 km (return trip at mid-day) in a rural area as model for delivery trip. The route passes the Weser mountains with many avenues and hills in Lower Saxony, Germany, at ($51^{\circ} 59' \text{ N}$, $9^{\circ} 31' \text{ E}$). It also passes through many small villages such as Emmerthal and Bodenwerder. The daily procedure includes 1) the outward trip to ISFH at ≈ 5 am, 2) parking and PV charging at ISFH, 3) the return trip at ≈ 12 am, 4) parking and PV charging at home, 5) charging by grid overnight. By this, the full day can be exploited for measurements. During parking at ISFH (at home), the front of the vehicle points in the direction of 355° (330°) while 0° equals north. The main driving direction during the outward (return) trip is north (south).

Sol. RRL **2022**, 6, 2100516

irradiation.^[14] Harvesting all of this radiation would have allowed for 18.8 kWh for our given module efficiency and module area.

3. Results

Table 1 lists the main quantities extracted from the data logged during procedure steps (1)–(4) with a total measurement time of 12.5 h and a total driven distance of 60.6 km. A couple of stops implied the lower average velocity at home drive.

The measured (time-averaged) irradiation up to 830.5 W m^{-2} at noon (roof) and the measured temperature up to 23.2°C is consistent with the stationary measurements.^[14] During the home drive at noon, the sum of the time-averaged irradiation on both sides and on the rear corresponds to 53 % of the time-averaged irradiation on the roof. During parking and PV charging, the sum of the irradiation on the sides and on the rear is even larger than the irradiation on the roof.

Figure 3 shows the time-resolved measurement data from the irradiation sensors. The irradiation on the roof mainly reflects the elevation of the sun, while irradiation on the sides is also affected by the azimuth angle and the respective orientation of the vehicle. From a comparison of right/left during parking, it is confirmed that the orientation of the vehicle is similar during parking at ISFH and at home. During parking, the sky was clear since no effects of clouds are resolvable. During driving, transient shading effects occurred. The steep increase in the irradiation measured on the roof and on the right-hand side of the vehicle at the beginning of the “parking and PV-charging @ ISFH”-section, as well as the steep fall in the irradiation measured on the roof and on the left-hand side of the vehicle at the end of the “parking and PV-charging @ home”-section is caused by shading of the sensors from the surroundings.

When integrating the module power at the input side of the MPPTs over the measurement time, we obtain a total energy yield of 11.4 kWh for this day. As pointed out in ref. [15], also in our case the lion's share of the energy is harvested during parking. The difference in the harvested energy is mainly implied by the different durations of the periods. But even when comparing the time-averaged total power, the value during home drive at noon (0.92 kW) is slightly lower than during parking and charging at home (1.03 kW). This is despite of the fact that the time of day for the latter implies a lower irradiation. Since we can exclude the occurrence of clouds for the home drive at this day, this difference is most likely implied by shading effects during driving (see Figure 3) and/or by a more favorable orientation of the vehicle during parking. During the home drive at noon, the contribution of the sides and the rear to the energy yield is 35.9%. During parking at ISFH, however, sides (mainly right-hand) and rear contributed 45.5% of the energy yield at the input side of the MPPTs.

At the output side of the MPPTs, we obtain a total energy yield of 10.1 kWh for this day. Thus, the ratio of the energy transferred by the MPPTs is 88.4%. Obviously, the MPPTs wired to modules on the roof perform more efficient: on the output side on the MPPTs, the contribution of the roof to the total energy yield is larger than its contribution at the input side of the MPPTs. Indeed, a detailed analysis reveals that the efficiency of the MPPTs wired to modules on the roof (on the sides) is 95% (75%).

Around 60% of output energy of the MPPTs is stored immediately in LV buffer battery. At no point in time, the LV buffer battery was fully charged (SoC not listed here). This is, among others, a consequence of the fact that also the HV battery was not fully charged and thus capable of storing further PV-converted energy. When assigning an “efficiency” to the LV buffer battery, one has to note that charging and discharging is not performed simultaneously. Rather, discharging is performed within discrete time intervals, and could also involve energy which was stored at a former point in time (compare drive to ISFH). Nevertheless, averaging over the entire course of the day should give a fair estimation. On the exemplarily test day, the difference between the total energy stored in and discharged from the LV buffer battery was 0.6 kWh. We furthermore notice that the amount of energy received at the LV side of the DC/DC is by 1.5 kWh smaller than the amount of energy released at the output side of the MPPTs. When taking into account a storage loss of 0.6 kWh in the LV buffer battery, further 0.9 kWh “are missing.” We associate this energy with the operation of the electronics of the VIPV system (Microautobox, data logger, cooling, power supply of DC/DC, and so on). The amount of energy directly transferred from the MPPTs to the DC/DC without intermediate storage (4.1 kWh in total) is calculated from the difference of the output energy of the MPPTs and the energy stored in the LV buffer battery.

For the essential DC/DC, our analysis reveals that in total 25 energy packages were transferred from the LV to the HV level at this test day. The average transfer duration for an energy package was 605 s. The DC/DC was, therefore, active during 33.7% of the total time. Obviously, this value increases with increasing irradiation since the LV buffer battery is charged sufficiently more quickly. When comparing the energy released on the HV side (7.7 kWh) with the energy received on the LV side (8.6 kWh), the average DC/DC conversion efficiency is 90%.

When furthermore relating the total energy released on the HV side of the DC/DC (7.7 kWh) to the total energy at the (LV) input side of the MPPTs (11.4 kWh), we can assign a chain efficiency for all VIPV components of 68.6%.

Eventually, we relate the PV-converted energy that was released at the HV side of the DC/DC to the energy consumption of the vehicle. Among many other channels of the Controller Area Network (CAN), the SoC of the HV battery and thus, for its given capacity of 40 kWh, the change in the stored energy, is recorded. For the measurement during parking at ISFH (at home), there is a difference between the amount of energy fed into the HV battery by DC/DC and the stored energy of 0.4 kWh (0.8 kWh). Besides losses during charging, this difference is implied by parasitic energy consumption, most likely by the active vehicle (ignition on = lights on, power steering on, and so on). For future vehicle generations, this parasitic energy consumption can be mitigated by avoiding the necessity of an active board net during PV charging. During driving, the SoC of the HV battery decreases despite of PV charging—simply because PV can only provide a fraction of the energy required for driving. Again, a comparison of the energy released at the HV side of the DC/DC and the SoC allows for a calculation of the energy outflow from the HV battery due to driving and parasitic consumption and its relation to the driven distance. The resulting average energy consumption is 21.3 kWh/100 km. When

Table 1. Results obtained within the four measurement periods—drive to ISFH, parking and PV charging at ISFH, drive home, parking and PV charging at home—at the test day May 31, 2021.

	Drive to ISFH	Parking and PV charging @ ISFH	Drive to home	Parking and PV charging @ home	Average	Sum
Start time measurement (Central European Time)	03:55	04:44	10:45	11:44		
Measurement duration [s]	2189.7	21 622.2	3534.5	17526.3		44872.7
<i>Drive data</i>						
Time average velocity [km h ⁻¹]	49.6	0	31	0		
Driven distance [km]	30.1	0	30.4	0		60.6
<i>Irradiation and temperature</i>						
Time average irradiation roof [W m ⁻²]	32.5	597.6	830.5	695.7		
Time average irradiation left [W m ⁻²]	21.1	68.7	145.7	514.3		
Time average irradiation right [W m ⁻²]	105.7	561.0	206.9	139.9		
Time average irradiation rear [W m ⁻²]	55.7	253.8	85.7	179.3		
Time average ambient temperature [°C]	6.9	16.6	20.9	23.2		
<i>Modules (input side of MPPTs)</i>						
Total energy yield of all modules [kWh]	0.0	5.5	0.9	5		11.4
Contribution of modules on the roof to energy yield [%]	17.7	54.5	74.1	58.4	51.2	
Contribution of modules on the left to energy yield [%]	5	3.8	8.3	29.9	11.7	
Contribution of modules on the right to energy yield [%]	62.2	34.8	14.4	7.0	29.6	
Contribution of modules on the rear to energy yield [%]	15.2	7	3.3	4.8	7.6	
<i>MPPTs (output side)</i>						
Total energy yield of all MPPTs [kWh]	0.0	4.9	0.8	4.4		10.1
Contribution of MPPTs wired to modules on the roof to energy yield [%]	26.6	58	78.9	63.3	56.7	
Contribution of MPPTs wired to modules on the left side to energy yield [%]	2.8	2.8	7.3	28.9	10.4	
Contribution of MPPTs wired to modules on the right side to energy yield [%]	58.5	33.2	12	4.3	27	
Contribution of MPPTs wired to modules on the rear to energy yield [%]	12.1	6	1.9	3.5	5.9	
<i>LV buffer battery</i>						
Total energy stored in LV buffer bat. [kWh]	0	3	0.5	2.6		6
Total energy discharged from LV buffer bat. [kWh]	0.3	2.5	0.5	2.2		5.4
Energy directly transferred from MPPTs to DC/DC (w./o. intermediated storage in LV buffer bat.) [kWh]	0	1.9	0.4	1.8		4.1
<i>DC/DC</i>						
Number of energy packages transferred into the HV battery by DC/DC	1	14	2	8		25
Fraction of time with DC/DC active [%]	21.6	33.4	36.7	35.5	33.7 ^{a)}	
Amount of energy released on HV side [kWh]	0.2	3.6	0.7	3.2		7.7
Amount of energy received on LV side [kWh]	0.3	4	0.7	3.6		8.6
Efficiency of DC/DC [%]	89.2	89.9	90.5	90	89.9	
<i>Chain efficiency (electronic components) and range extension</i>						
Chain efficiency [%]		66.5	75	64.2	68.6	
Change in State of Charge of HV battery [%]	−15	8	−15	6		
Change in energy stored in HV battery according to SoC [kWh]	−6	3.2	−6	2.4		
Further parasitic energy consumption [kWh]		0.4		0.8		
Energy consumption for driving (not correct for further parasitic consumption) [kWh/100 km]	20.7		21.9		21.3	

Table 1. Continued.

	Drive to ISFH	Parking and PV charging @ ISFH	Drive to home	Parking and PV charging @ home	Average	Sum
Energy consumption for driving (correct for further parasitic consumption) [kWh/100 km]	19.8		19.5		19.6	
Range extension (PV from entire day, not corrected for further parasitic consumption) [km]					36.3	
Range extension (PV from entire day, corrected for further parasitic consumption) [km]					42.3	

^{a)}This value is not the mean value of the single measurement sections (with different durations). It is the ratio of the sum of all DC/DC = active time periods and the total measurement duration.

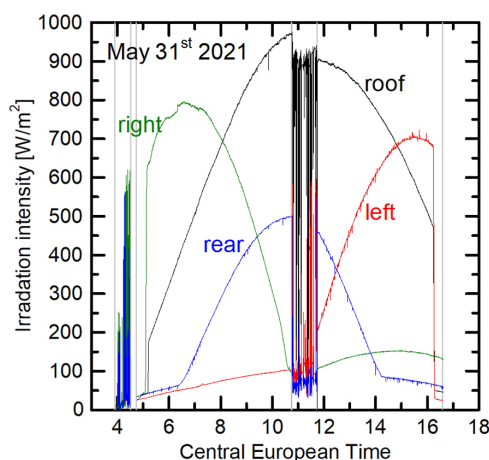


Figure 3. Time-resolved irradiation as measured by the sensors on the roof, and the sides and on the rear on May 31, 2021. The vertical gray lines indicate the four different measurement sections drive to ISFH, parking and PV-charging at ISFH, drive to home, parking and PV-charging at home.

assuming that the parasitic energy consumption can be mitigated also during driving, a correction (We calculate an average parasitic power consumption during parking. This value is multiplied by the duration of the drives and subtracted from the difference between the energy released at the HV side of the DC/DC and the energy stored in the HV battery according to its SoC) yields an energy consumption for pure driving of 19.6 kWh/100 km. This value is very close to the specification of Streetscooter of 19.2 kWh/100 km. Relating the 21.3 kWh/100 km to the energy fed into the HV battery by the DC/DC (7.7 kWh), the net range extension (not corrected for the current parasitic consumption) achieved on this test day was 36 km.

4. Discussion

4.1. Harvested Energy, Efficiencies, and Optimization Potential

When comparing the 11.4 kWh harvested at the input side of the MPPTs with the abovementioned upper estimation of 18.8 kWh when assuming that all modules are facing the sun (which is of course not the case), this can be considered as a promising result.

Furthermore, this value agrees with our expectations based on previous irradiation measurements on driving vehicles^[16] for comparable locations. For more southern locations, irradiation and thus harvested energy would be significantly higher.

The average efficiency of the MPPTs wired to modules mounted on the roof—95%—is comparable to that of state-of-the-art MPPTs for stationary systems,^[17] and meets the assumptions drawn in refs. [4,18]. One possible explanation for the fact that the MPPTs wired to modules mounted on the sides and the rear are performing by $\approx 20\%$ less efficient could be that these devices have to track the maximum power point of two modules in series. The resulting higher voltages, and, due to lower irradiation, the lower current might be further away from the optimum operating point of the MPPTs. Another hypothesis is that the higher frequencies measured for the transient shading on the sides as compared with the roof^[15] may compromise the maximum power point tracking.

To our knowledge, this is the first report on the average DC/DC conversion efficiency actually measured in field tests. The obtained value of 90% meets well the assumptions drawn in refs. [4,18].

The obtained chain efficiency of 68.6% is an already promising result for the first test of our prototype. It is not too far from the assumed value of 73.9% from ref. [4]. Nevertheless, it is obvious that each single component as well as the DC/DC conversion strategy can be optimized further.

The range extension actually achieved on May 31, 2021 is already more than half of the daily driven distance, implying that every second grid-charging event can be omitted under these weather conditions. Mitigating the parasitic energy consumption would increase the range extension to 42 km. Further improvements could be achieved by increasing the chain efficiency of the electronic components—the total energy at the input side of the MPPTs would have enabled a range extension of 58 km at the test day. Last but not least, a more complete utilization of the available area on the compartment— $\approx 15 \text{ m}^2$ instead of the 11.6 m^2 covered so far with “essential” parts of the PV modules—would roughly scale the total energy harvested at the input side of the MPPTs to 14.7 kWh (17.8 kWh) for the current (future 23% efficient) modules. For the latter case, range extension between 51 and 62 km for the current and a perfect chain efficiency of the electronic components could be achieved. Both a more complete utilization of the area of the compartment as well as an increase in the module efficiency could be for example achieved by the

shingling technique. Furthermore, the power consumption for driving can possibly also be reduced in future VIPV vehicle generations, e.g., by implementing light weight foil-based modules rather than glass-based modules. One should note that a commercial vehicle in real use would also have additional payload—which makes it even more important to utilize as light as possible modules.

4.2. Estimation of Reduction in CO₂ Emissions

Last but not least, we tried to estimate the implied reduction of CO₂ emissions compared with a pure grid-based charging for the actual results obtained on May 31, 2021. This is not trivial, since the CO₂ emissions of the German grid mix are constantly decreasing and vary within the course of a day. While—mainly thanks to stationary PV—at noon in April 2020, an average emission down to 167 g CO₂/kWh is reported,^[19] the emissions increased to values above 300 (450) g CO₂/kWh at night in April 2020 (November 2020). This is a supporting argument for VIPV, since electrically driven vehicles—in particular commercial ones—are mainly connected to the grid during night. Thus, the actual CO₂ emissions accompanied with grid charging—and thus the potential of VIPV to reduce the emissions—are likely higher than calculated from average values for CO₂ emissions of the grid mix. Since we do not want to specify a certain driving profile here, we nevertheless assume 350 g CO₂/kWh as an average value for the German grid mix in 2020. Also, the emissions associated with on-board PV energy conversion are difficult to assess. For stationary PV, 46 g CO₂/kWh^[20] have been reported in 2012 while recent values are probably lower. However, PV systems on vehicles have a shorter lifetime (8 rather than 30 years) and receive less irradiation than stationary PV systems. Accordingly, Kanz et al.^[2] have calculated at least ≈150 g CO₂/kWh for a VIPV system on a LCV (“green scenario,” ≈670 kWh expected annual VIPV contribution [roof only], ≈80% chain efficiency). Thus, a zero-order approximation for the saved CO₂ emissions on our exemplary test day results in 11.4 kWh · 200 g less CO₂/kWh = 2.3 kg less CO₂.

However, it is also fair to remark that the difference of ≈150 g CO₂/kWh for a VIPV system^[2] to 46 g CO₂/kWh for a stationary PV system^[20] would suggest to charge from the latter to minimize the CO₂ emissions. Even if one takes into account that a further stationary battery would be required to enable overnight charging, the corresponding additional CO₂ emissions—≈20 (≈28) g CO₂/kWh for a battery produced in Europe (China)^[21,22]—do by far not compensate this difference. This comparison is of course too simplifying—first, because the deployment of stationary PV has not yet progressed to an extent that every electrically driven vehicle can be charged from it, and second because it disregards further aspects like land use, consumer convenience, and so on. Nevertheless, it points on the necessity to further reduce the CO₂ emissions implied by the production of VIPV systems. Indeed, the calculations in ref.[2] refer to a PV production in China. If PV production in countries with a low CO₂ emission factor of the grid becomes reality, the difference between the CO₂ emissions implied by VIPV and stationary PV will shrink. We think that for a decarbonization of all sectors including transport, both approaches—the installation of as

much stationary PV as possible and a deployment of VIPV—can contribute.

5. Conclusion

For our practical demonstration LCV with integrated PVs, we study the energy flow from irradiation, modules, MPPTs, low-voltage buffer battery to HV battery via DC/DC, and eventually for driving for an exemplarily test drive day (May 31, 2021). These insights are facilitated by logging numerous data from sensors, batteries, and electronic VIPV components. One essential part of our demonstrator vehicle is the DC/DC converter from 12 to 400 V, which was found to operate with an efficiency of 90 %. The chain efficiency of the electronic components from the input side of the MPPTs to the HV output side of the DC/DC was 68.6%. The range extension obtained at this exemplarily test day on our test route (51° 59' N, 9° 31' E) was 36 km, the corresponding CO₂ savings account for ≈2.3 kg. For our daily driving distance of 60.6 km, the corresponding solar coverage factor on May 31, 2021 factor was 60%. We discussed possibilities to increase the range extension to >60 km, which, at least for the given weather conditions, would cover completely our daily energy consumption. One should also note that for future generations of the electronic components, a more compact design will be targeted, e.g., by integrating all MPPTs into a multichannel device.

We will continue to perform our daily test drives until end of 2021. By this, data averaged over the respective months will be recorded, allowing for a conclusive assessment of the annually averaged solar coverage factor and for a comparison with predictive models. Not less relevant is the durability of all components, in particular with regards to the effects of mechanical stress (vibrations, shocks, hail, and so on) on the PV modules. We will regularly check the status of the modules integrated into the vehicle based on fluorescence and luminescence measurements.

Acknowledgements

The authors thank the German Federal Ministry for Economic Affairs and Energy for funding this work under grant FKZ 0324275 (Street), and the state of Lower Saxony for institutional funding. The authors especially thank Continental Engineering Services (CES, Nordostpark 30, 90411 Nuremberg)—Robert Steib, Andreas Semmelmann, and Stefan Lutz—for their dedicated and excellent work on the integration of the VIPV components into the vehicle. The authors also thank Sascha Wolter for his help with the data analysis, Dirk Bartels for his work on the grid charging point, and Annika Raugewitz for her contributions to the planning of the test drives. Furthermore, the authors thank the IEA PVPS task 17 team, in particular Keiichi Komoto, for inspiring discussions.

Open access funding enabled and organized by Projekt DEAL.

Conflict of Interest

The authors declare no conflict of interest.

Data Availability Statement

Research data are not shared.

Keywords

demonstrator vehicles, energy flow analysis, test drives, vehicle-integrated photovoltaics

Received: July 8, 2021

Revised: October 12, 2021

Published online: November 14, 2021

- [1] <https://skysolar.co.nz/1912-baker-electric-car/> (accessed: November 2021).
- [2] O. Kanz, A. Reinders, J. May, K. Ding, *Energies* **2020**, *13*, 5120.
- [3] A. Sierra Rodriguez, T. de Santana, I. MacGill, N. J. Ekins-Daukes, A. Reinders, *Prog. Photovolt. Res. Appl.* **2020**, *28*, 517.
- [4] NEDO, PV-Powered Vehicle Strategy Committee Interim Report, <https://www.nedo.go.jp/content/100885778.pdf> (accessed: November 2021).
- [5] Press release from May 7th 2021, <https://sonomotors.com/en/press/press-releases/sono-motors-and-man-truck-bus-want-to-jointly-analyze-applications-of-solar-technology-in-commercial-vehicles/> (accessed: November 2021).
- [6] Press release from June 22nd 2021, <https://www.electrive.com/2021/06/22/tropos-tests-van-with-integrated-solar-panels/> (accessed: November 2021).
- [7] Press release from July 13th 2020, <https://www.pv-magazine.com/2020/07/13/midsummer-unveils-500-w-rooftop-panel/> (accessed: November 2021).
- [8] Press release from Oct. 8th 2020, <https://www.scania.com/group/en/home/newsroom/news/2020/truck-trailers-with-solar-panels-can-save-fuel.html> (accessed: November 2021).
- [9] Press release from Sep. 19th 2018, <https://www.dhl.com/global-en/home/press/press-archive/2018/dpdhl-group-now-charges-trucks-with-a-natural-energy-source.html> (accessed: November 2021).
- [10] A. J. Carr, E. van den Tillaart, A. R. Burgers, T. Köhler, B. K. Newman, in *Proc. of the 37th European Photovoltaic Solar Energy Conf. and Exhibition*, WIP GmbH & Co Planungs-KG, Munich, Germany **2020**, pp. 1701–1705.
- [11] M. Yamaguchi, T. Masuda, K. Araki, D. Sato, K.-H. Lee, N. Kojima, T. Takamoto, K. Okumura, A. Satou, K. Yamada, T. Nakado, Y. Zushi, Y. Ohshita, M. Yamazaki, *Prog. Photovolt. Res. Appl.* **2021**, *29*, 684.
- [12] This area is occupied with components essential for the function of the modules (cells, intercell spacing, interconnectors, and so on). The total area available on the compartment is even larger (15 m²). Using half- or even shingled cells would allow to also cover the so far wide white module edges visible in Figure 1a.
- [13] The magnetic sensor is installed to monitor the orientation of the vehicle—which of course has implications on the illumination on the different surfaces. For a future analysis, we plan to correlate the time-resolved orientation during driving to the measured time-dependent illumination from each sensor, and to compare it with advanced optical models. Here, the orientation during parking reported below is measured with the magnetic sensor.
- [14] https://www1.muk.uni-hannover.de/hp-design2020/wetter_archiv_frame.html (accessed: November 2021).
- [15] K. Araki, Y. Ota, T. Masuda, D. Sato, M. Yamaguchi, in *PVSEC-29 Proc.*, **2019**, pp. 2592–2598.
- [16] G. Wetzel, L. Salomon, J. Krügener, R. Peibst, High time resolution measurement of solar irradiance onto driving car body for vehicle integrated photovoltaics, **2021**, submitted for publication.
- [17] D. P. Hohm, M. E. Ropp, *Prog. Photovolt. Res. Appl.* **2003**, *11*, 47.
- [18] K. Araki, L. Ji, G. Kelly, M. Yamaguchi, *Coatings* **2018**, *8*, 251.
- [19] <https://www.eupd-research.com/co2-emissionen-im-deutschen-strommix-schwanken-im-jahresverlauf-2020-sehr-stark/>.
- [20] <https://www.nrel.gov/docs/fy13osti/56487.pdf>.
- [21] G. Bieker, Global Comparison Of The Life-Cycle Greenhouse Gas Emissions of Passenger Cars, ICCT White Paper, International Council on Clean Transportation Europe, Berlin **2021**.
- [22] Ref. [21] reports on 60 (68) kg CO₂ per kWh battery capacity for a battery produced in Europe (China). We furthermore draw the assumption here that such a stationary battery allows for 3000 charging/discharging cycles during its lifetime.